Removal of Evans Blue by using Nickel-Iron Layered Double Hydroxide (LDH) Nanoparticles: Effect of Hydrothermal Treatment Temperature on Textural Properties and Dye Adsorption

Fatiha Boukraa Djellal Saiah,[*1] *Bao-Lian Su,*[2] *Noureddine Bettahar*[1]

Summary: The use of low-cost adsorbent has been investigated as a replacement for the current expensive methods of removing dyes from wastewater. The sorption of acid dye (Evans Blue) from aqueous effluents onto anionic clays (hydrotalcite-like) has been studied. Hydrotalcite may be an effective adsorbent of organic molecules due to its hydrophobic nature and the accessibility of its interlayer region. Ni/Fe layered double hydroxide (LDH), with a molar ratio of 3, were synthesised by coprecipitation followed by hydrothermal treatment at different temperatures (85, 100 and 140 °C) for 4 days. The materials were characterised by X-ray powder diffraction (XRD), infrared spectroscopy, scanning electron microscopy (SEM), transmission electron microscopy (TEM), and N_2 adsorption-desorption (BET). The diffractograms and FT-IR spectroscopy of the fresh materials showed that the hydrotalcite is present in all samples. The XRD pattern obtained was typical of a hydrotalcite, where the interlayer anion is CO_3^{2-}, XRD and Infrared spectroscopy complemented each other by showing that with treatment the degree of order increased regardless of the type of treatment. Furthermore, it was shown that aging at increased temperature and pressure increased crystallinity. TEM showed that crystal size increased with aging temperature, so that growth occurred on the edges resulting in the formation of hexagonal plate shaped hydrotalcite crystals. The surface area decreased with increasing the hydrothermal treatment temperature. The effects of various parameters such as hydrothermal treatment temperature, crystallite size, contact time and calcination on the extent of adsorption were investigated. The studies of the removal efficiency of the reactive textile dye: Evans Blue (Direct Blue 53) by $NiFeCO_3$ HDLs showed that the effect of hydrothermal treatment temperature on adsorption increases with aging temperature. The Evans Blue (EB) removal percent increased with increasing contact time. Above the 70%, 50% and 20% of EB adsorption occurred in the first 2 min for HDL-140, HDL-100 and HDL-85°C respectively. Furthermore, it was found that the calcined materials are much more effective than the original LDH in removing Evans Bleu dye from an aqueous solution.

Keywords: adsorption kinetics; anionic clays; dye; hydrothermal treatment; TEM

Introduction

Dyes usually have a synthetic origin and complex aromatic molecular structures which make them more stable and more difficult to biodegrade.[1] Dyes can be classified as follows[2]: (a) anionic: direct, acid, reactive dyes; (b) cationic: basic dyes; and (c) non-ionic: disperse dyes. Color

[1] Laboratory of Physics-Chemistry of Materials: Catalyse and Environment, University of Sciences and Technology of ORAN "Mohamed Boudiaf" USTO.MB, B.P. 1505 El Menaouer, Oran 31000, Algeria
E-mail: f_boukraa2003@yahoo.fr
[2] Laboratory of Inorganic Materials Chemistry (CMI), University of Namur (FUNDP), 61 Rue de Bruxelles 5000 Namur, Belgique

removal from effluent is one of the most difficult requirements faced by the textile finishing, dye manufacturing, and pulp and paper industries. These industries are major consumers of water and therefore cause water pollution. The discharge of these to the river stream without proper treatment causes irreparable damage to the crops and living beings, both aquatic and terrestrial.[3] Many investigators have studied different techniques for removal of colored dye from wastewater, e.g. chemical coagulation/flocculation, different advanced oxidation processes,[4,5] ozonations,[6,7] cloud point extraction,[8] nanofiltration,[9] micellar enhanced ultrafiltration,[8] and adsorption onto: (i) agricultural solid waste,[10] (ii) calcined alunite,[11] (iii) various types of activated carbon[12,13] and(iv) surfactant impregnated montmorillonite,[14] etc. Due to the low biodegradability of dyes, a conventional biological wastewater treatment process is not very efficient in treating a dye wastewater. It is usually treated by physical, chemical or biological treatment processes.[15–18] Adsorption on activated carbon has been found to be an effective process for dye removal from dye wastewater, but it is too expensive.[19] Low-cost absorbents developed to replace activated carbon generally have low adsorption capacities. New economical, easily available and highly effective adsorbents are still needed. One such promising material is the family of synthetic compounds called hydrotalcites or hydrotalcite-like compounds or layered double hydroxides.[20] Hydrotalcite may be an effective adsorbent of other organic molecules due to its hydrophobic nature and the accessibility of its interlayer region.[21] The most famous class is Mg–Al hydrotalcites with the general formula $[Mg^{2+}_{1-x}Al^{3+}_{x}(OH)_2]^{x+}[A^{n-}_{x/n}.\ mH_2O]^{x-}$; where A^{n-} is an n-valent anion and x can have values between 0.15 and 0.34.[22] Their structure consists of positively charged brucite-like layers, $(Mg_{1-x}M^{3+}_{x}(OH)_2)^{x+}$, alternating with negatively charged inter layers containing anions and water molecules $(X^{n-}_{x/n}.\ H_2O)^{x-}$[23,24]

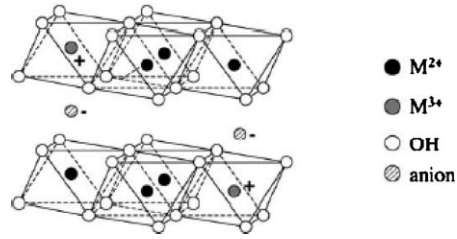

Figure 1.
Crystal structure of the hydrotalcite-like compounds.

(Figure 1).The interlayer anions and water molecules can be exchanged with other anions, so hydrotalcites are theoretically good anionic exchangers.[25] Various LDH compounds can be synthesized with several preparation methods. In general, the most commonly used method is coprecipitation at various or constant pH, followed by aging at a given temperature.[26–28] Hydrothermal treatment generally increases crystallinity, depending mainly on the temperature although pressure and time also are important parameters. Miyata found, by hydrothermally treating a Mg/Al hydrotalcite, that the temperature of treatment had a dramatic effect on crystallite size, such that size increased up to 180 °C but decreased above 200 °C.[22] A more recent study investigated the effect of varying time but maintaining a constant temperature.[24,29,30] This study found by X-ray diffraction and infrared spectroscopy that the order in the inter layer region and the cristallinity in the hydroxide layer increased with time. Furthermore by using transmission electron microscopy, it was shown that the average size of the lamellar hexagonal particles increased with aging time.[30] In the present work we report on the preparation of Nickel Iron carbonated hydrotalcite followed by hydrothermal treatment at different temperature for 4 days. Adsorption of Evans Bleu dye (Bleu Direct 53), anionic dye (molecular structure is given in Figure 2), on $NiFeCO_3$ has been studied. The effect of the structural and morphological properties of this adsorbent on the dye sorption

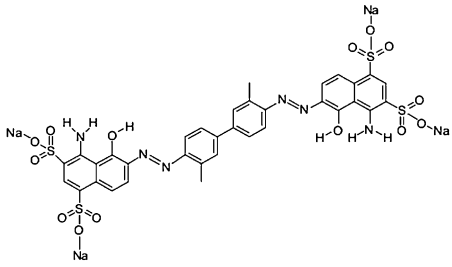

Figure 2.
Chemical structure of Evans Bleu (EB) dye.

capacity according to hydrothermal treatment temperature and calcination has been explored. The experimental data were analyzed using various kinetic models, and kinetic constants were evaluated.

Experimental Part

Preparation

All reactants used in this work have high purity degree and were from Aldrich. A co-precipitation method was used to prepare $NiFeCO_3$ LDHs with a molar ratio $Ni/Fe = 3$. In a typical synthesis, the samples were obtained by dropwise adding, at room temperature, a solution containing 1.5 mol $NiCl_2.6H_2O$ and 0.5 mol $FeCl_3.6H_2O$ dissolved in 250 ml of distilled water to a vigorously stirred solution (250 ml) containing 1M NaOH and 2M Na_2CO_3 at constant $pH = 11$. The suspension obtained was stirred for a further 1 hour at room temperature. The suspension was then divided into several equal portions, to undergo different hydrothermal treatments. The content was then transferred into the Teflon coated stainless steel autoclave in order to obtained better crystallized materials.[31]These portions, denoted $NiFeCO_3$85, $NiFeCO_3$100 and $NiFeCO_3$140 were aged at 85, 100 and 140 °C for 4 days. The precipitate formed was filtered and washed several times in distilled water to remove excess free ions, until pH of the filtrate was 7, followed by drying at 60 °C overnight. Part of the resulting material was calcined at 320 °C for 2 h to obtain calcined LDH labelled $CNiFeCO_3$.

Characterization

Powder X-ray diffraction patterns (XRD) of synthesized LDHs were recorded using Phillips PW´1820 with Cu-Kα radiation ($\lambda = 1{,}5418$ Å) over a 2θ range of 4-70°. Identification of the crystalline phases was by comparison with the JCPDS files.[32] FT-Infrared spectra of materials were recorded using KBr pellets technique in a Perkin-Elmer FT-IR 2000 spectrometer in the range of 4000–400 cm^{-1}. Specific surface area was measured in a Micromeritics Tristar 3000 by nitrogen adsorption-desorption (77K) after degassing the sample by flowing nitrogen at 100 °C overnight. The surface areas were determined by applying the BET method to the nitrogen adsorption data. The pore diameter and the pore size distribution were determined by the BJH method.[33] The morphology of the obtained phases was studied using a Philips XL-20 Scanning electron microscope (SEM) at 20 keV. Electron micrographs of the samples were taken by the transmission electron microscopy (TEM) on a Philips TECNAI-10 instrument at 80 keV.

Dye Adsorption Experiments

A sorption kinetic study of Evans Blue (EB) on Nickel-Iron LDH were carried out by adding 250mg of $NiFeCO_3$ LDH or calcined compound into 100ml of EB solution at concentration about 50 mg/l. The mixture was stirred at room temperature at 400 rpm. An approximately 5 ml of the solution was withdrawn at desired time intervals, ranging from 2 to 70 min, and then centrifuged at 6500 rpm for 10 min. EB equilibrium concentration was analysed using a Perkin-Elmer UV-Vis spectrometer at $\lambda_{max} = 605$ nm. This conditions hold for all materials displayed above. The effects of hydrothermal treatment temperature for the sorption of EB onto these materials were also investigated.

Results and Discussion

Hydrothermally Treated Samples

The X-ray diffraction patterns are shown in (Figure 3). The patterns of all samples showed the diffraction lines typical for hydrotalcite structure with interlayer carbonate.[34] As shown in Figure 3, the XRD patterns of LDH samples consist of two first sharp and symmetrical peaks with some asymmetrical peaks at high angle, indicating their good crystallinity.[35,36] The sharpness and the intensity of (003) and (006) reflection planes of the two first peaks (Figure 3) were considered to be proportional to the crystallinity and the crystallite size of material. The results have been explained by a structural rearrangement and probably a better packing of the layers introduced by the increase of the hydrothermal treatment temperature conditions. The positions and relative intensities of the maxima for our samples are coincident with those reported in the literature for reevesite, $Ni_{0.75}Fe_{0.25}(CO_3)_{0.125}(OH)_2$ 0.38 H_2O (JCPDS file 40-0215).[37] The cell constant c is commonly calculated as c = 3d (003), assuming a 3R polytipism for the hydrotalcite,[38,39] while the value of the cell constant a is calculated as a = 2 d(110).[28] This parameter corresponds to the minimum cation-cation distance in the brucite-like layers and is related to the position of the peak corresponding to planes (110).

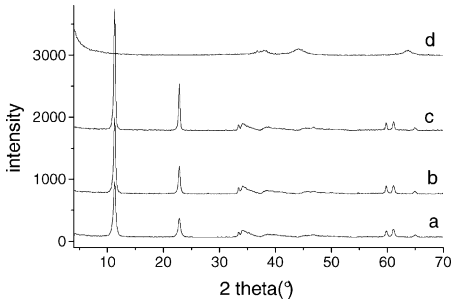

Figure 3.
X-ray diffraction patterns of $NiFeCO_3$ LDHs at different hydrothermal treatment temperature: a = 85 °C, b = 100 °C, c = 140 °C; and d = CNiFeCO3 calcined product.

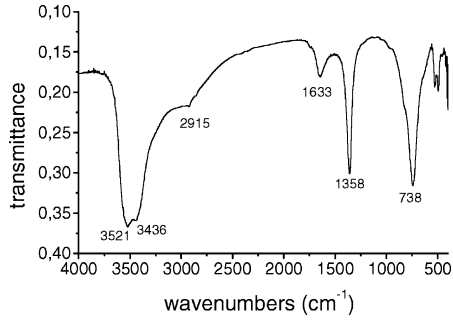

Figure 4.
Infrared spectra of $NiFeCO_3$140.

The FT-IR spectrum is shown in Figure 4. All samples show similar spectra with a broad absorption band centred at 3436 cm^{-1} assigned to ν(OH) stretching modes of free and hydrogen-bonded hydroxyl groups and water molecules, whose bending mode is responsible for the medium-intensity band at 1633 cm^{-1}.[40] The strong absorption band at 1358 cm^{-1} is due to the vibration mode of the interlayer carbonate anions. It was shown that ν_3 mode of CO_3^{2-} species in all samples are recorded as a single peak, this indicating that this moiety preserves its D_{3h} symmetry. The bands in the 800-400 cm^{-1} range are due to lattice vibrations, mainly involving transationnal motions of oxygen ions in the layers.

All nitrogen adsorption isotherms correspond to type II in the IUPAC classification, originating from adsorption on mesopore samples.[41] The values of the specific surface area (S_{BET}) of the samples are included in Table 1. It can be seen that the surface area decreased with increasing treatment temperature, and thus a much lower adsorption capacity for sample $NiFeCO_3$140 is observed. This suggests to nonuniform size with aggregates of plate-like particles leading to slit-shaped pores of the hydrotalcite material.[42] This is the conclusion reached from the analysis of the transmission electron microscopy in Figure 5. Sample $NiFeCO_3$85 (Figure 5a) appears as very small particles. They can be seen as stacks of lamellar hexagonal particles with an average size close to

Table 1.
Textural properties of the LDHs and calcined precursor.

Samples	LDH		
	S_{BET} [a]	Vp [b]	Dp [c]
	m^2/g	cm^3/g	Å
$NiFeCO_3$85	72	0.49	137
$NiFeCO_3$100	47	0.46	198
$NiFeCO_3$140	26	0.19	145
$CNiFeCO_3$	150	0.18	50

[a] Specific surface area.
[b] Cumulative pore volume.
[c] Pore diameter.

20–150 nm. These results, together with those from nitrogen adsorption, indicate that the hydrothermal treatment temperature has led to sintering and cristalization of the samples, thus accounting for the higher degree of symmetry in the sample hydrothermally treated at high temperature (average crystallite size close to 100-500 nm), as suggested by XRD and FT-IR results presented above. The SEM images of $NiFeCO_3$ LDH (Figure 6) show a well-developed platelet structure. A sponge-type structure is exhibited due to the overlapping of such platelets. The SEM images of the materials showed a gradual crystallization during the increase of hydrothermal treatment temperature. Thin hexagonal flat crystals in a layered structure are more formed in $NiFeCO_3$140 sample (Figure 6c).

Calcined Compounds

As it is known, one of the most interesting uses of hydrotalcites is as precursor for preparation of well dispersed mixed oxides. The $NiFeCO_3$140 was calcined for 2 hours at 320 °C. This sample is named as CNi-$FeCO_3$ and has been characterized by XRD, texture assessment by nitrogen adsorption and transmission electron microscopy. As shown in Figure 3, the XRD patterns showed that the layered structure of $NiFeCO_3$ is destroyed by heating it at 320 °C, resulting in mixed oxide NiFeO (periclase-like structure) indicating removing of carbonate. Calcination at this temperature leads to a profile with only three broad reflections. These peaks recorded at $2\theta = 37°$ due to plane (111), at $2\theta = 43°$ due to plane (200), and at $2\theta = 63°$ due to plane (220). These positions coincide with the main diffraction maxima of NiO nickel oxide (JCPDS file 4-0835), which is badly crystallized. All calcined samples showed similar curves. The BET surface area of calcined samples increased by a factor of 3 to 4 upon hydrothermal treatment conditions. This can be explained assuming that removal of

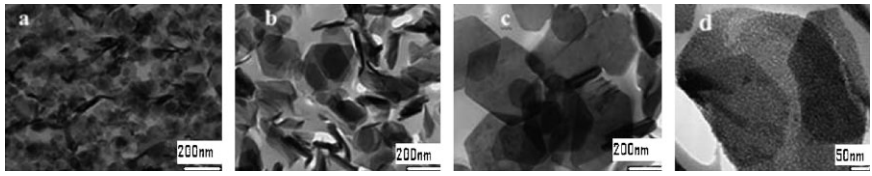

Figure 5.
TEM micrographs of sample $NiFeCO_3$ hydrothermally treated for 4 days at: (a) 85 °C, (b) 100 °C and (c) 140 °C and (d) $CNiFeCO_3$ calcined sample at 320 °C

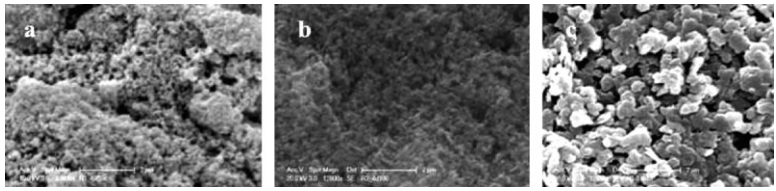

Figure 6.
SEM micrographs of sample $NiFeCO_3$ hydrothermally treated for 4 days at: (a) 85 °C, (b) 100 °C and (c) 140 °C.

water molecules and carbon dioxide from carbonate in the interlayer during calcination leads to formation of channels and pores, thus accounting for the increase in specific surface area.[43] These results are confirmed from the analysis of the transmission electron microscopy in (Figure 5d). The structure of calcined samples is still crystalline, with crystals of different size, which demonstrate highly porous particles (Figure 5d).

Removal Dye Performance

Effect of Contact Time

Effect of sorption time on EB removal by $NiFeCO_3$ LDH, at different hydrothermally treatment temperature, is shown in Figure 7. The dye percentage adsorbed (%) was calculated using the following equation:

$$\text{Removal dye}\% = \frac{C_0 - C_e}{C_0} \cdot 100 \qquad (1)$$

where C_0 and C_e were the initial and equilibrium concentrations (mg/L) of the dye in solution, respectively. q_t was calculated at t using the following equation:

$$q_e(C_0 - C_e)\frac{V}{m} \qquad (2)$$

where V and m were the volume of the dye solution (mL) and the mass of adsorbent (mg), respectively.

(Figure 7A) shown that the EB removal percent increased with increasing contact time. More than 70%, 50% and 20% of EB adsorption occurred in the first 2 min for $NiFeCO_3140$, $NiFeCO_3100$ and $NiFeCO_385$ respectively. The sorption rate increases with an increase in hydrothermal treatment temperature; it correlates with the increase of crystallite size, crystallinity and the structure's form of dye. The sorption of this dye occur via different mechanisms, because Evans Blue has four sulfonic groups ($-SO_3$) and an anthraquinone ring in its molecular structure while, the hydrothermally treated $NiFeCO_3$ at high temperature has low surface areas and act as partitioning media in the sorption.[44] Similar results are also observed for sorption capacity (Figure 7B). The sorption capacity at equilibrium increases from 20 to 24 mg/g with an increase in the hydrothermal treatment temperature from 85 to 140 °C. The equilibrium time of the EB sorption was 50, 48 and 46 minutes at 100% of sorption for $NiFeCO_385$, $NiFeCO_3100$ and $NiFeCO_3140$ respectively.

Effect of Calcination

It has been shown that calcined products $CNiFeCO_3$ exhibit a high sorption capacity. The adsorption reached equilibrium at the first 5 min with uptake percent of 100% (Figure not shown). It can be explained by the increase of the surface area and surface basicity of materials. In order to studies the controlling mechanism of adsorption process, a sorption kinetic study of Evans Blue (EB) on $CNiFeCO_3$ was carried out by EB solution at concentration about $C_0 =$ 100 mg/L (Figure 8). The equilibrium time of the EB sorption onto $CNiFeCO_3$ was reached after 40 minutes with an uptake of 100% and a sorption capacity of 43.5 mg/g.

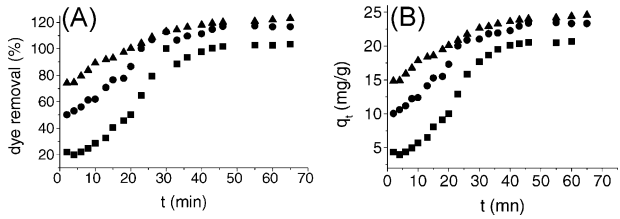

Figure 7.
Effect of hydrothermal treatment: (A) on dye removal, (B) on adsorption capacity of sample $NiFeCO_3$ treated for 4 days at: ■ = 85 °C, ● = 100 °C and ▲ = 140 °C, reaction conditions: $T = 24$ °C, $C_o = 50$ mg/L

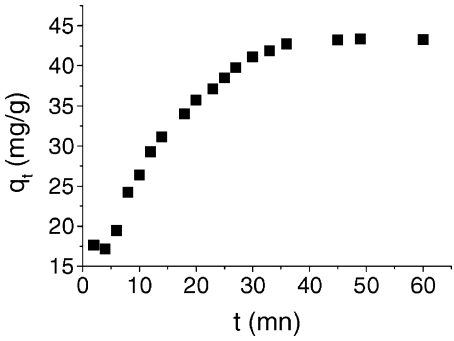

Figure 8.
Effect of calcinations on adsorption capacity of sample $CNiFeCO_3$, reaction conditions: $T = 24\,^{\circ}C$, $C_0 = 100$ mg/L.

Kinetic Models of Adsorption

Most sorption processes take place by a multistep mechanism comprising: (i) diffusion across the liquid film surrounding the solid particles (a process controlled by an external mass transfer coefficient), (ii) diffusion within the particle itself assuming a pore diffusion mechanism (intraparticle diffusion) and (iii) physical or chemical adsorption at a site.[45]

The controlling mechanism of adsorption process of Evans Blue on $NiFeCO_3$ treated at different hydrothermal temperatures was analysed using the Lagergren first-order kinetic model and the pseudo-second-order model.[46–48] The Lagergren first-order model was given by the equation:

$$\log(q_e - q_t) = \log q_e - \frac{k_1}{2.303} t \qquad (3)$$

where q_t and q_e represent the amount of dye adsorbed (mg/g) at any time t and at equilibrium time, respectively, and k_1 the adsorption rate constant (mn^{-1}). k_1 and q_e can be obtained from the intercept and slope of the plot of $\log(q_e - q_t)$ vs. t (Figure not shown). In this equation, it is necessary to know q_e from Figure 7B. The q_e values obtained from the first-order kinetic equation did not agree with the experimental q_e values, which indicate that the adsorption of Evans Blue by $NiFeCO_3$ does not follow the first –order rate kinetic.

The pseudo-second-order model was given by the following equation:

$$\frac{t}{q_t} = \frac{1}{k_2 q_e^2} + \frac{t}{q_e} \qquad (4)$$

where k_2 is the adsorption rate constant. k_2 and q_e can be obtained from the intercept and slope of the plot of (t/q_t) vs. t (Figure 9).

The initial sorption rate can be obtained as q_t/t approaches zero:

$$h = Kq_e^2 \qquad (5)$$

where h is the initial sorption rate (mg/g mn).

A comparison of calculated and experimental results for the adsorption onto $NiFeCO_3$ is shown in Table 2. It was seen that experimental data fitted pseudo second-order equation for $NiFeCO_3140$, $NiFeCO_3100$ and $CNiFeCO_3$ with high correlation coefficient values (R^2) (Figure 9). The equilibrium sorption capacity (q_e) calculated was slightly more reasonable than that of the pseudo-first-order when compared to the experimental q_e values ($q_{e(exp)}$) (Table 2). This suggests that the adsorbents studied belongs to the second-order kinetic model, based on the assumption that the rate limiting step may be chemical or chemisorption involving valency forces through sharing or exchange of electrons between adsorbent and dye. Similar phenomena

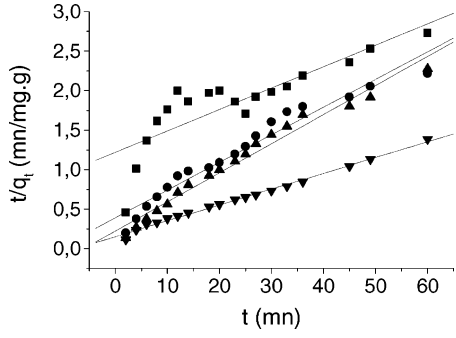

Figure 9.
Pseudo-second-order kinetic plots for the adsorption of EB onto uncalcined HDL: ■ = $NiFeCO_385$, ● = $NiFeCO_3100$, ▲ = $NiFeCO_3140$; reaction conditions: $T = 24\,^{\circ}C$, $C_0 = 50$ mg/L. Calcined HDL: ▼ = $CNiFeCO_3$; $T = 24\,^{\circ}C$, $C_0 = 100$ mg/L.

Table 2.
kinetic parameters for the adsorption of Evans Bleu onto $NiFeCO_3$ HDL hydrothermally treated at various temperatures and calcined precursor.

samples	$q_{e(exp)}$	k_2	h	q_t	R^2	k_p	R^2
	(mg/g)	(g/mg mn)	(mg/g mn)	(mg/g)		(mg/g mn$^{1/2}$)	
$NiFeCO_3$85	20.5	$0.55\,10^{-3}$	0.82	38	0.740	3.36	0.947
$NiFeCO_3$100	23.4	$4.33\,10^{-3}$	3.13	27	0.990	2.49	0.901
$NiFeCO_3$140	24.0	$8.53\,10^{-3}$	5.78	26	0.997	1.68	0.960
$CNiFeCO_3$	43.5	$2.3\,10^{-3}$	5.99	51	0.997	4.95	0.900

have also been observed in biosorption of RB 2, RY 2 and Remazol black B dye on biomass[49] and for the adsorption of Congo red on activated carbon.[50] This model indicates that the adsorption of EB onto $NiFeCO_3$85 may be followed from 30 mn up to 1 hour. The initial sorption rate h (Eq. (5)) increases from 0.82 to 5.99 mg/g.mn with the increase of hydrothermal treatment temperature of $NiFeCO_3$. This is due to a higher driving force that should result in a more rapid change in the rate at which Evans Blue is adsorbed initially onto $NiFeCO_3$ HDL. The pseudo second-order rate constant, k_2, was also following this trend.

In order to examine the suitability of intra-particle diffusion in fitting our data, the rate constant diffusion was given by the following equation[51]:

$$q_t = k_p t^{1/2} \quad (6)$$

where k_p is the intra-particle diffusion rate constant (mg/g mn$^{1/2}$). The k_p values were obtained from the slope of the straight-line portions of plots of q_t vs. $t^{1/2}$ (Figure 10). The values are given in Table 2. The results show that increasing hydrothermal temperature increased the intra-particle diffusion rate constant(Table 2). Plots do not pass through the origin. This is indicative of some degree of boundary layer control and this further indicates that the intra-particle diffusion is not the only rate-limiting step, but also other kinetic models may control the rate of adsorption. The correlation coefficients (R^2) for the intra-particle diffusion model are lower than that of the pseudo-second order model. The diffusion model indicates that the adsorption of EB onto $NiFeCO_3$85 and $CNiFeCO_3$ may be followed by this model up to 20 and 35 min. respectively. According to the previous results, it can be conclude that surface adsorption and intra-particle diffusion were concurrently operating during the $NiFeCO_3$ LDH and Evans Blue interactions.

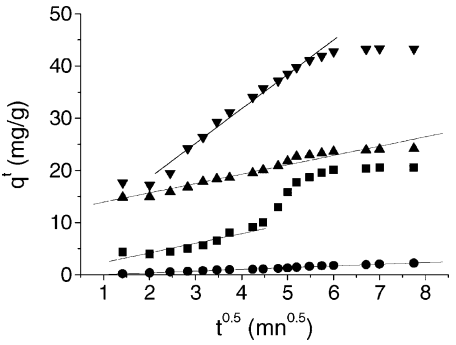

Figure 10.
Intraparticle diffusion model for the adsorption of EB at hydrothermally treated HDL: ■ = $NiFeCO_3$85, ● = $NiFeCO_3$100, ▲ = $NiFeCO_3$140; and calcined precursor: ▼ = $CNiFeCO_3$.

Conclusion

This study investigates the equilibrium and kinetic adsorption of Evans Blue dye on nickel iron anionic clays hydrothermally treated at various temperatures and calcined precursor. The effect of hydrothermal conditions on structural and textural properties was studied in the temperature range 85–140 °C for 4 days. The cristallinity of the samples was observed to increase on increasing the hydrothermal treatment temperature. This gives rise to the decrease of the specific surface area from 72 to 26 m^2/g. SEM and

TEM results showed an apparent growth of the particles with increasing treatment conditions. A well developed layered and platelet structure of the NiFe hydrotalcite was observed from the SEM image. TEM images revealed the regular hexagonal plate morphology.

The percentage of eliminated Evans Blue dye was found to depend on the hydrothermal treatment conditions and the calcination of the adsorbent. The NiFe LDH was able to remove from 22 to 72% of dye solutions at 50 mg/L in the first 2 min, according to hydrothermal treatment conditions. The calcined materials are much more effective than the original LDHs in removing Evans bleu dye from an aqueous solution.

The results indicate that the pseudo-second-order model is the most suitable to describe the adsorption kinetics of EB on $NiFeCO_3$ LDH. The experimental $q_{e(\exp)}$ values slightly agree with the calculated ones obtained from the pseudo-second-order kinetics model. This indicates that the adsorption of the solid phase is in agreement with a chemisorption mechanism being the rate-determining step. The adsorption of EB onto $NiFeCO_385$ and $CNiFeCO_3$ may be followed by an intra-particle diffusion model for 20 and 35 min. respectively.

[1] S. Seshadri, P. L. Bishop, A. M. Agha, *Waste Manage* **1994**, *15*, 127.
[2] G. Mishra, M. Tripathy, *Colourage* **1993**, *40*, 35.
[3] C. O'Neill, F. R. Hawkes, D. L. Hawkes, N. D. Lourenco, H. M. Pinheiro, W. Delee, *J. Chem. Technol. Biotechnol.* **1999**, *74*, 1009.
[4] P. K. Malik, S. K. Saha, *Sep. Purif. Technol.* **2003**, *31*, 241.
[5] U. Bali, *Dyes Pigments* **2004**, *60*, 187.
[6] C. Wang, A. Yediler, D. Lienert, Z. Wang, A. Kettrup, *Chemosphere* **2003**, *52*(7), 1225.
[7] A. Bes-Pia', J. A. Mendoza-Roca, L. Roig-Alcover, A. Iborra-Clar, M. I. Iborra- Clar, M. I. Alcaina-Miranda, *Desalination* **2003**, *157*(1–3), 81.
[8] M. K. Purkait, S. DasGupta, S. De, *Sep. Purif. Technol.* **2004b**, *37*(1), 81.
[9] S. Chakraborty, M. K. Purkait, S. DasGupta, S. De, J. K. Basu, *Sep. Purif. Technol.* **2003**, *31*, 141.
[10] S. Rengaraj, S. H. Moon, R. Sivabalan, B. Arabindoo, V. Murugesan, *Waste Manage* **2002**, *22*, 543.
[11] M. Ozacar, I. A. Sengil, *J. Hazard. Mater. B* **2003**, *98*, 211.
[12] Y. Al-Degs, M. A. M. Khraisheh, S. J. Allen, M. N. A. Ahmad, *Sep. Sci. Technol.* **2001**, *36*(1), 91.
[13] P. R. Jana, S. De, J. K. Basu, *Chem. Eng. J.* **2003**, *95*, 143.
[14] J. H. Bae, D. I. Song, Y. W. Jeon, *Sep. Sci. Technol.* **2000**, *35*(3), 353.
[15] I. M. Banat, P. Nigam, D. Singh, R. Marchant, *Bioresour. Technol.* **1996**, *58*, 217.
[16] W. Dellee, C. O'Neil, F. R. Hawkes, H. M. Pihneiro, *J. Chem. Technol. Biotechnol.* **1998**, *73*, 23.
[17] K. Skelly, *Rev. Prog. Coloration* **2000**, *30*, 21.
[18] T. Robinson, G. MucMullan, R. Marchant, P. Nigam, *Bioresource Technol.* **2001**, *77*, 247.
[19] A. S. Ozcan, A. Ozcan, *J. Colloid Interf. Sci.* **2004**, *276*, 39.
[20] T. Sato, T. Wakabayashi, M. Shimada, *Ind. Eng. Chem. Prod. Res. Dev.* **1986**, *25*, 89.
[21] T. Toraishi, S. Nagasaki, S. Tanaka, *Appl. Clay Sci.* **2002**, *22*, 17.
[22] S. Miyata, *Clays and Clay Minerals* **1980**, *28*, 50.
[23] T. Kawabata, Y. Shinozuka, Y. Ohishi, T. Shishido, K. Takaki, K. Takehira, *J. Mol. Catal. A-Chem.* **2005**, *236*, 206.
[24] W. T. Reichele, *Solid State Ionics* **1986**, *22*, 135.
[25] M. Bellotto, B. Rebours, O. Clause, J. Lynch, D. Bazin, E. Elkaım, *J. Phys. Chem.* **1996**, *100*, 8535.
[26] P. S. Braterman, Z. P. Xu, F. Yarberry, in: "*Layered Materials Handbook*", S. M. Auerbach, K. A. Carrado, P. K. Dutta, Eds., Marcel Dekker, New York **2004**, p. 373.
[27] V. Rives, Ed. Layered Double Hydroxides: Present and Future, Nova Science Publishers, New York **2001**.
[28] F. Cavani, F. Trifiro, A. Vaccari, *Catal. Today* **1991**, *11*, 173.
[29] L. Hickey, J. T. Kloprogge, R. L. Frost, *J. Mat. Sci.* **2000**, *35*, 4347.
[30] W. T. Reichele, S. Y. Kang, D. S. Everhardt, *J. Catal.* **1986**, *101*, 352.
[31] F. M. Labajos, V. Rives, M. A. Ulibarri, *J. Mater. Sci.* **1992**, *27*, 1546.
[32] JCPDS: Joint Committee on Powder Diffraction Standards, International Centre for Diffraction Data, Pennsylvania, U.S.A. **1977**.
[33] E. P. Barrett, L. G. Joyner, P. P. Halenda, *J. Am. Chem. Soc.* **1951**, *73*, 373.
[34] F. Thevenot, R. Szymanski, P. Chaumette, *Clays Clay Miner.* **1989**, *37*, 396.
[35] Y. You, H. Zhao, G. F. Vance, *Appl. Clay Sci.* **2002**, *21*, 217.
[36] M. A. Ulibarri, Pavlovic, C. Barriga, M. C. Hermosin, J. Cornejo, *Appl. Clay Sci.* **2001**, *18*, 17.
[37] A. Mendiboure, R. Schollhora, *Rev. Chem. Miner.* **1986**, *23*, 819.
[38] A. S. Bookin, V. I. Cherkashin, A. Drits, *Clays Clay Miner.* **1993**, *41*, 558.
[39] A. S. Bookin, A. Drits, *Clays Clay Miner.* **1993**, *41*, 551.

[40] J. M. Hernandez-Moreno, M. A. Ulibarri, J. L. Rendon, C. J. Serna, *Phys. Chem. Minerals* **1985**, *12*, 34.
[41] K. S. W. Sing, D. H. Everett, R. A. W. Hall, L. Moscou, R. A. Pierotti, J. Rouquérol, T. Siemieniewska, *Pure and Appl. Chem.* **1985**, *57*(4), 603.
[42] S. Mohmel, I. Kurjawski, D. Uecker, D. Muller, W. Gebner, *Cryst. Res. Technol.* **2002**, *37*, 359.
[43] E. C. Kruissink, L. J. van Reijden, J. R. H. Ross, *J. Chem. Soc., Faraday Trans. 1* **1981**, *77*, 649.
[44] J.-F. Lee, M. M. Mortland, S. A. Boyd, C. T. Chiou, *J. Chem. Soc. Faraday Trans. 1* **1989**, *85*, 2953.
[45] K. V. Kumar, V. Ramamurthi, S. Sivanesan, *J. Colloid Interface Sci.* **2005**, *284*, 14.
[46] Y. S. Ho, G. McKay, *Process Saf Environ. Prot.* **1998**, *76*, 183.
[47] Y. S. Ho, G. McKay, *Process Biochem.* **1999**, *34*, 451.
[48] Y. S. Ho, C. C. Chiang, *Adsorption* **2001**, *7*, 139.
[49] Z. Aksu, *Biochem. Eng. J.* **2001**, *7*, 79.
[50] C. Namasivayam, D. Kavitha, *Dyes Pigments* **2002**, *54*, 47.
[51] W. J. Weber, J. C. Morriss, *J. Sanitary Eng. Div. ASCE* **1963**, *89*, 31.

